ingegneria sismica
International Journal of Earthquake Engineering
Anno XLIII - Num. 2 - 2026

Study of power supply decision monitoring considering simulation modeling of delay jitter in IoT data

Yumin He[1,*], *Guobang Ban*[1], *Jing Gan*[1], *Guanghui Xi*[1], *Xinbiao Xiong*[1] *and Jiangang Liu*[1]

[1] Guizhou Power Grid Co., Ltd. Electric Power Research Institute, Guiyang, Guizhou, 550000, China

SUMMARY: *With the wide application of Internet technology in smart grid, the time delay jitter of user-side data has caused serious interference to the accuracy of power supply decisions. This paper establishes a delay analysis model based on tandem queuing system, observes the queue at the moment of service packet arrival, and adopts the strategy of analyzing one by one to obtain the probability generating function of delay jitter for real-time class service packets. On this basis, a power supply decision monitoring system based on IoT communication is constructed, which collects real-time data of power supply through 4G/fiber optic communication and MV carrier network, and realizes optimal scheduling and decision making of power supply with the help of reinforcement learning algorithm. The experimental results show that compared with the optimal trend and genetic algorithm, the reinforcement learning-based algorithm proposed in this paper has faster convergence speed and higher stability, and its economy is better than the comparison algorithm, and its total cost is reduced by more than 2000 yuan. The practicality of the algorithm in this paper in coping with communication delay and user-side data fluctuation is verified.*

KEYWORDS: *CSMA/CA; Reinforcement Learning Algorithm; Real-Time Class Service Package; Delay Jitter; Power Supply Decision*

1 Introduction

Driven by the digital economy and “peak carbon and carbon neutral”, the hub position of the power supply system in the construction of a new type of power system is becoming more and more prominent, and it plays a key role in assisting the transformation and development of the electric power industry and guaranteeing energy efficiency [1, 2]. When the Internet of Things (IoT) technology is applied, wireless sensors can be installed in the smart grid in order to real-time monitoring of the power energy long-distance transmission process, by obtaining the dynamic changes in cable temperature and current value, timely detection and resolution of grid faults, and provide a reliable guarantee for the safe and stable supply of power energy [3-5]. In the power supply system, IoT devices collect the voltage, current, frequency and other data of the power supply to carry out tasks such as power supply state assessment, fault identification, power supply load prediction, etc., to realize real-time monitoring and decision-making guidance for the power supply system [6-8]. With the high percentage penetration of distributed new energy, high percentage access of power electronic equipment, high integration of power and electronic equipment, and the emergence of multiple production and marketing users, it brings profound changes and major challenges to the technical

*heyumin1980@163.com
https://doi.org/10.65102/is2026697
Published: 30 April, 2026

characteristics, operation mechanism, and development mode of power supply and IoT [9, 10]. Among them, the IoT data delay jitter problem is worthy of attention.

Data delay refers to the time elapsed from the sending of a data packet to its destination. It includes several factors such as propagation delay, transmission delay, queuing delay and processing delay [11]. Secondly, delay jitter is an unstable manifestation of network delay, which measures the variation of packet delay during transmission. Delay jitter can be caused by several factors, such as network congestion, transmission errors, and routing changes [12, 13]. The higher delay jitter indicates the worse stability of IoT and the reliability of packet transmission is reduced, which is manifested as data loss and duplication [14-16]. While the problem of delay jitter is often neglected in traditional power supply decision monitoring, simulation modeling of it can explore the impact of delay jitter on power supply decision monitoring as well as improve the effectiveness of power supply decision monitoring. Therefore, simulation modeling of IoT data delay jitter in power supply decision monitoring is necessary.

This paper establishes a delay analysis model based on a case-by-case analysis strategy, through which the characteristics of data delay and jitter are portrayed. Based on this, a reinforcement learning-based power supply decision monitoring system is constructed. The system consists of application layer, platform layer, communication network layer and perception layer, and adopts B/S architecture and bus transmission protocol information to complete the adaptive control of power supply decision-making system in FTTB scenario. The system introduces a reinforcement learning algorithm for sequential decision-making and long-term optimization with a small amount of information, which is applied to deal with power supply decision scheduling containing delay fluctuations. The performance of the algorithm in this paper is verified through simulation experiments and comparison tests in various aspects such as convergence and economy.

2 Simulation modeling of delay jitter based on IoT data

The existence of non-real-time class of service packets in wireless access networks is bound to have an impact on the service of real-time class of service packets, which further makes the performance of real-time class of service packets with delay jitter change. The arrival characteristics of the two types of service packets are random; and due to the collision between packets in the CSMA/CA network, the service time of the packets is also random. These two points make it difficult to analyze the delay jitter of real-time class of service packets. In this chapter, we adopt the delay jitter analysis method. In order to analyze the delay jitter of real-time class service packets, the queue is first observed at the moment of its arrival and the delay of real-time class service packets is analyzed. Then the time delay of the packet is analyzed time slot by time slot within the arrival interval of the real-time class service packet and the time delay expression of the real-time class service packet is obtained. Finally, in the probabilistic generation domain, the probabilistic generation function for the delay jitter of real-time class service packets is obtained.

2.1 System model

A common communication scenario for a wireless access network contains M nodes and an AP. the nodes use the CSMA/CA mechanism for data transmission with the AP. Each node in the network contains real-time class service packets and non-real-time class service packets. The two types of service packets in each node enter the queue sequentially, and the service rule for packets is first-come-first-served. We abstract the process of accessing real-time class

service packets and non-real-time class service packets in a node to the wireless network into a queuing model as shown in Fig. 1. The same random access parameters are used for both types of service packets. In this chapter, we assume that: each node is within the carrier listening range of the rest of the nodes and there are no obstacles in the listening area, so the hidden node problem is not considered.

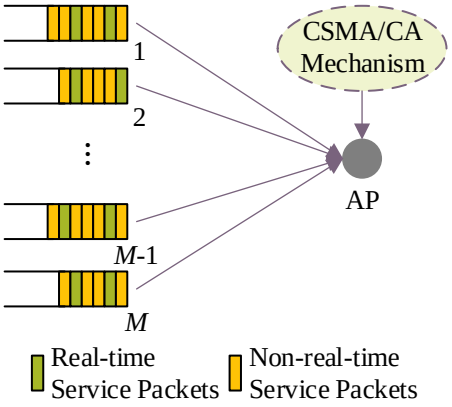

Figure 1: The queuing model for wireless access in heterogeneous business scenarios

2.2 CSMA/CA mechanism

2.2.1 CSMA/CA modeling

The IEEE802.11 protocol standard uses the CSMA/CA mechanism to transmit packets. Referring to the previous work of the laboratory, the CSMA/CA mechanism is modeled as a two-dimensional discrete-time Markov chain, and the detailed analysis process is described in Ref. Based on Markov theory, the expression of $b_{0,0}$ can be obtained by derivation as follows:

$$b_{0,0}=\begin{cases}\dfrac{2(1-2p)(1-p)}{W_0\left(1-(2p)^{\alpha+1}\right)(1-p)+(1-2p)\left(1-p^{\alpha+1}\right)} & \alpha\le m\\ \dfrac{2(1-2p)(1-p)}{W_0\left(1-(2p)^{m+1}\right)(1-p)+(1-2p)\left(1-p^{\alpha+1}\right)} & \alpha>m\\ +2^m W_0 p^{m+1}(1-2p)\left(1-p^{\alpha-m}\right) & \end{cases} \tag{1}$$

where W_0 is the initial backoff window range, m is the maximum backoff order, and α is the maximum number of retransmissions.

The probability τ that a packet is transmitted in any time slot can be expressed as:

$$\tau=\frac{1-p^{\alpha+1}}{1-p}b_{0,0} \tag{2}$$

The probability p of a packet collision is:

$$p=1-(1-\tau)^{M-1} \tag{3}$$

2.2.2 Analysis of hours of service

In this section, we analyze the service time of packets. During the backoff process, a time slot is maintained with $(1-p)$ count decrement, the original state is maintained with p_e for T_s time, and the original state is maintained with $(p-p_e)$ for T_c time. Then $L_d(z)$ denotes the PGF of the time required for the decreasing of the recession counter can be expressed as:

$$L_d(z)=(1-p)z+p_e z^{T_s}+(p-p_e)z^{T_c} \tag{4}$$

where $p_e=(M-1)\tau(1-\tau)^{M-2}$.

Let $L_i(z)$ be the PGF of the time required for the recession counter to decrement to zero when the recession order is i, which can be expressed as:

$$L_i(z)=\begin{cases}\dfrac{1}{W_i}\sum_{j=0}^{W_i-1}L_d^j(z), & i\le m\\ \dfrac{1}{W_m}\sum_{j=0}^{W_m-1}L_d^j(z), & i>m\end{cases} \tag{5}$$

The PGF of packet service time can be expressed as:

$$G(z)=(1-p)z^{T_r}\sum_{i=0}^{\alpha}\left(\left(pz^{T_r}\right)^i\prod_{j=0}^{i}L_j(z)\right)+\left(pz^{T_r}\right)^{\alpha+1}\prod_{j=0}^{\alpha}L_j(z) \tag{6}$$

2.3 Delay and Jitter Performance Simulation Analysis

In the next simulation, the packet delay and jitter performance of real-time class services are investigated in different scenarios by taking the real-time class service arrival interval obeying a fixed-length distribution and the non-real-time class service as a Poisson arrival process as examples.

2.3.1 Delay performance simulation in different scenarios

In this paper, we study the complementary cumulative distribution function of delay and discuss the packet delay performance from the following aspects.

(1) The effect of total network load intensity on packet delay performance

In this section, we first conduct a related study on the tandem queuing system, configuring the total load intensity of the system to be 0.5, 0.6,0.7,0.8, respectively, in which the average arrival rate ρD of real-time class services is set to 0.3 and kept constant, and the service rule is random acceptance of services. The simulation results of end-to-end delay performance of node 1 and tandem queuing system under four load intensities are shown in Fig. 2, and the delay performance with total load intensities of 0.5,0.6,0.7,0.8 are shown in Figs. (a)~(d), respectively, where the x-axis is the value of delay and the y-axis is the complementary cumulative distribution function of delay, which is represented in this paper in the form of a log-log plot.

In this paper, it is found that the complementary cumulative distribution function curves of time delay on the four graphs have the same trend, but the x-axis takes a different range of values, and the range of time delay is different. From figure (a) it is seen that when the total

network load is 0.5, the maximum delay of real-time class service at node 1 is 14 time slots, and the maximum end-to-end delay is 20 time slots, while in fact the probability that the delay at node 1 is greater than 6 time slots has been as low as 10-3, and the probability that the end-to-end delay is greater than 12 time slots is also less than 10-3, which indicates that the real-time class packet delay performance in this case is better. As the network load increases, the packet delay and end-to-end delay performance at node 1 deteriorates rapidly. Thus, in order to ensure the delay performance of real-time class services in real networks, appropriate traffic admission control mechanisms need to be designed in the network.

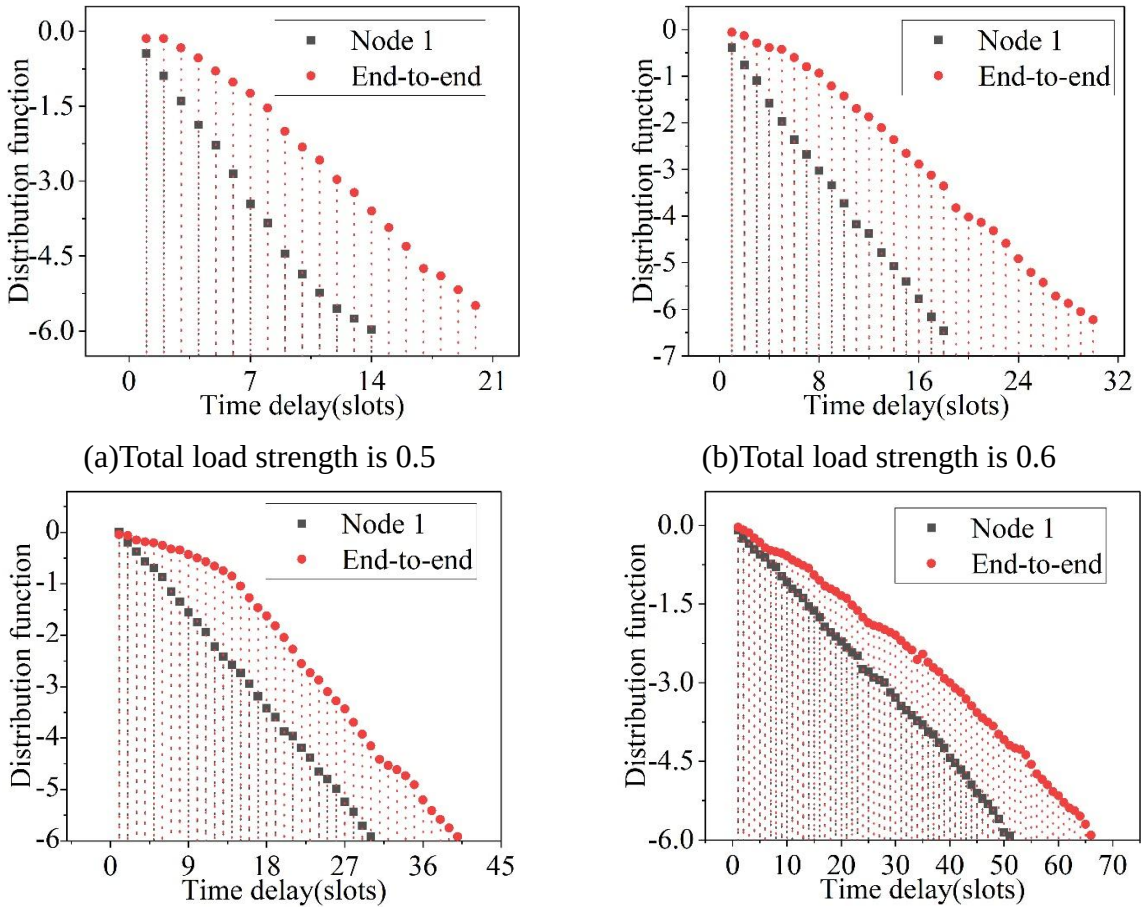

(a)Total load strength is 0.5

(b)Total load strength is 0.6

(c)Total load strength is 0.7

(d)Total load strength is 0.8

Figure 2: Delay performance simulation results

(2) Impact of service rules on packet delay performance

In this chapter, it is assumed that when the packets of real-time class services and non-real-time class services enter the system in the same time slot, there exist random service rules and prioritized service rules, and the impact of service rules on packet delay performance is investigated here. Configuring the total network load $\rho = 0.9$ and the real-time class service load $\rho D = 0.3$, the packet delay under the two service rules is compared, and Fig. 3 shows the delay performance comparison under the two service rules. Figures (a) and (b) show the comparison of node 1 delay performance and end-to-end delay performance, respectively.

The value of the packet delay complementary cumulative distribution function at the same point under the random service rule is always larger than the value under the prioritized service rule, indicating that the packet delay performance under the random service rule is

worse. It is also found that the difference between the delay curves under the two rules is not much, which is because this paper only assumes that when the packets of the two types of services enter the system in the same time slot, the two service orders will be distinguished, and when they do not enter the system in the same time slot, they still adopt the service rule of FIFO, and thus the difference between the curves is not too much.

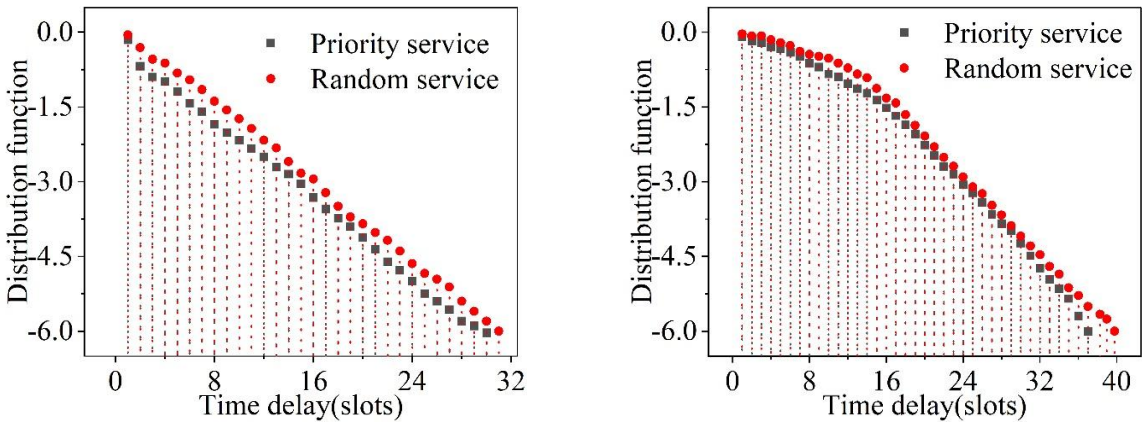

(a) Node 1 delay performance (b)End-to-end delay performance

Figure 3: The delay performance of the two service rules is compared

2.3.2 Simulation of jitter performance in different scenarios

In this section, the probability distribution function of the jitter of the real-time class of services at each tandem node is given. The simulation includes the following sections:

(1) Jitter performance under different load intensities

In this section, firstly, for a tandem queuing system with five nodes, the total load intensity of the system is configured to be 0.5,0.6,0.7,0.8, the average arrival rate ρD of real-time class services is set to be 0.3, and the service rule is to accept the services randomly. The simulation results of the probability distribution function of the jitter of real-time class services at each node under four load intensities are shown in Fig. 4, and the probability distribution function of the jitter with total load intensities of 0.5~0.8 are shown in Figs. (a)~(d), respectively.

Firstly, the probability distribution of jitter of each tandem node under the same load is compared. It is found that the probability distribution curves of node 1 and node 2 jitter are steeper near 5 time slots and the probability distributions are more concentrated, bounded by probability 0.05, and the jitter of node 1 and node 2 is mainly distributed between 2 and 7 time slots. The probability distribution curves of jitter at node 3 and node 4 are flatter, with jitter distributed between 1 and 10 time slots, which indicates that the jitter of packets takes more and more dispersed values as the number of nodes passing through increases in a tandem queuing system. Then comparing the probability distribution of jitter of the same node under different loads, it is found that the probability distribution of jitter of the same node takes more and more dispersed values as the total load of the network increases.

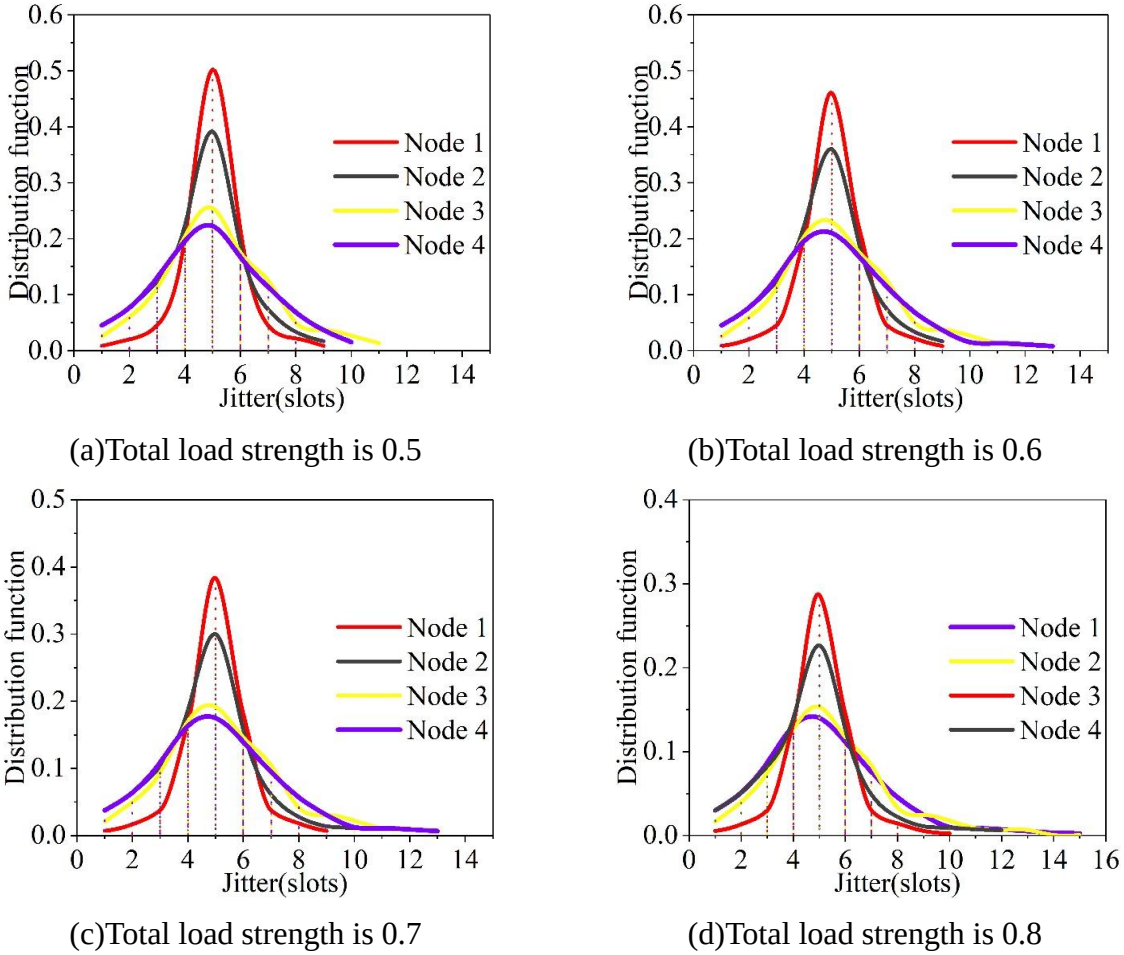

(a)Total load strength is 0.5 (b)Total load strength is 0.6

(c)Total load strength is 0.7 (d)Total load strength is 0.8

Figure 4: The impact of network load on jitter performance

(2) Jitter performance under different service rules

In this paper, we configure the total network load ρ=0.8 and the real-time class service load ρD=0.2, and simulate the probability distribution function of packet delay jitter of nodes 1,2,3,4 under the two rules of prioritized service and randomized service, respectively, and the impact of service rules on the jitter performance of each node is shown in Fig. 5, and the probability distribution of packet delay jitter of nodes 1,2,3,4 under the two rules of prioritized service and randomized service functions are shown in Figs. (a)~(d), respectively.

The probability distribution curve of packet jitter for the real-time class of service under the priority service rule is steeper near the 9 time slot, and the jitter is distributed with a greater probability near the 9 time slot. In contrast, the probability distribution curve of real-time class service under random service rule is flatter and jitter takes a more spread out value, but this gap slowly decreases as the number of passing nodes increases. Under the prioritized service rule, the real-time class of service packet jitter is only related to the change of system captain at its arrival moment. In contrast, under the random service rule, the packet jitter is not only related to the change of the system captain, but also related to the number of packets of the background flow that enters the system at the same time and may receive the service first, and thus the packet jitter takes a more dispersed value.

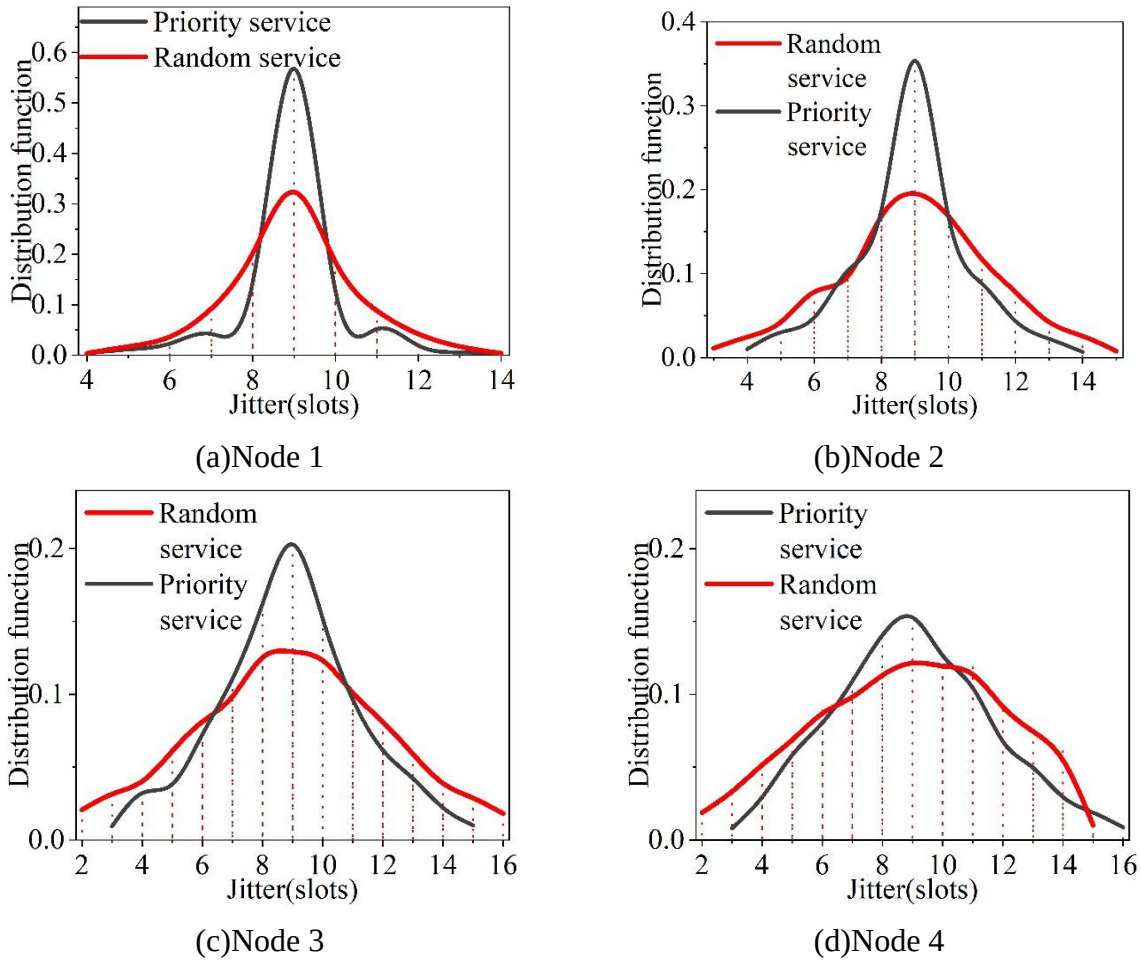

Figure 5: The effect of service rules on the shaking performance of each node

3 Reinforcement learning based power supply decision monitoring system construction

3.1 Analysis of the overall architecture and functional structure of the decision-making system

3.1.1 Overall architecture of the decision-making system

Power supply decision-making under FTTB scenario is carried out in embedded power system management mode, combined with the parameter distribution of power supply decision-making data under FTTB scenario, and temporal big data integration is carried out. Combined with statistical analysis methods, it realizes big data information management for power supply decision-making under FTTB scenario. According to the construction standards of the South China Network Internet of Things platform, the equipment collection device of the power supply decision-making system under FTTB scenario adopts the measurement data or strategy command control system, and based on the protocols provided by the platform, such as MQTT(s), CoAP, HTTP(s), GB/T28181, ONVIF, PG, etc., it builds the power supply decision-making system model. Access to build power supply decision-making system model. Based on the IoT platform architecture to establish the decision-making protocol model, through the video data transmission, to establish the joint control system structure model, to

converge the relevant data, the local networking form contains: micro-power wireless, Bluetooth, RS485, Ethernet, the overall architecture of the system's IoT is shown in Figure 6.

According to Figure 6 to establish the system architecture, using layered distribution structure design, the system consists of four layers: application layer, platform layer, communication network layer and perception layer. Adopting Web architecture system, under the temporal big data fusion technology, B/S architecture and bus transmission protocol are adopted to realize the informatization transmission and control of big data collection, and build the power supply decision-making and optimization control model under FTTB scenario as well as the cloud information processing library of parameter identification to realize the adaptive control of power supply decision-making system under FTTB scenario, and the overall architecture of the system is shown in Fig. 7.

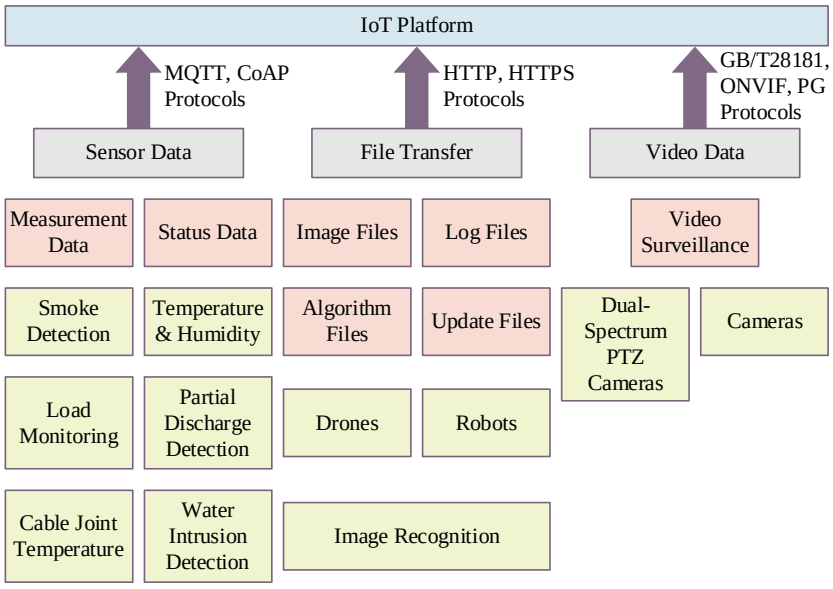

Figure 6: The overall architecture of the iot platform

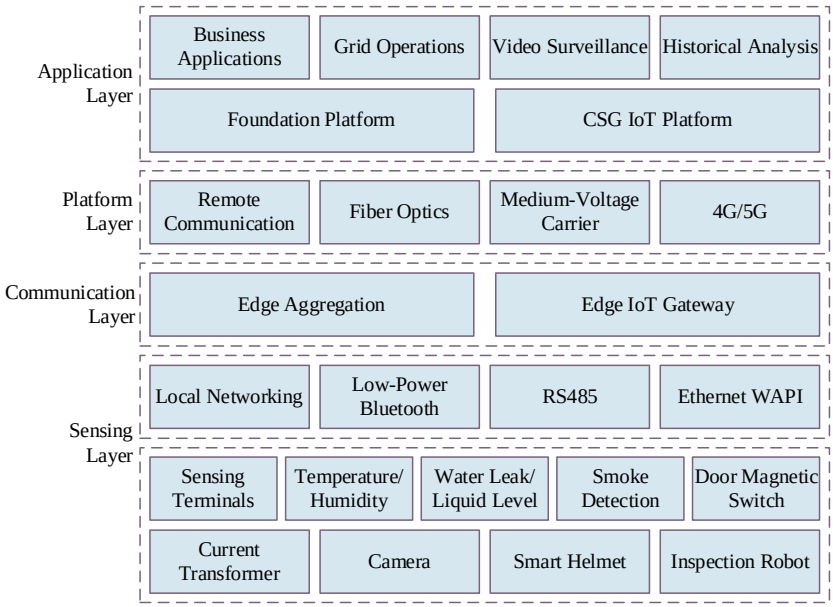

Figure 7: The overall structure of the power making system in FTTB scenario

3.1.2 Functional module analysis

According to the overall architecture of the system, the power supply decision-making system model containing five functional modules, namely, basic management, operation monitoring, video monitoring, alarm management, and comprehensive analysis, is constructed to realize the acquisition of relevant user and authority information of the system through the integration of the 4A platform of the power supply decision-making system in the FTTB scenario; it can also be realized through the platform itself for the transmission of information and the fusion of user information, and combined with the configuration of platform parameters, it can realize the configuration of the maintenance and management functions of the power supply decision-making system in the FTTB scenario. It can also realize the maintenance and management function configuration of the power supply decision-making system under FTTB scenario through information transmission and user information fusion by the platform itself, combined with the platform parameter configuration.

Adopting 4G/fiber optic communication and medium voltage carrier network, the power supply decision-making platform under FTTB scenario realizes page menu authority control through the configuration results, and obtains the functional module composition of the decision-making system as shown in Figure 8.

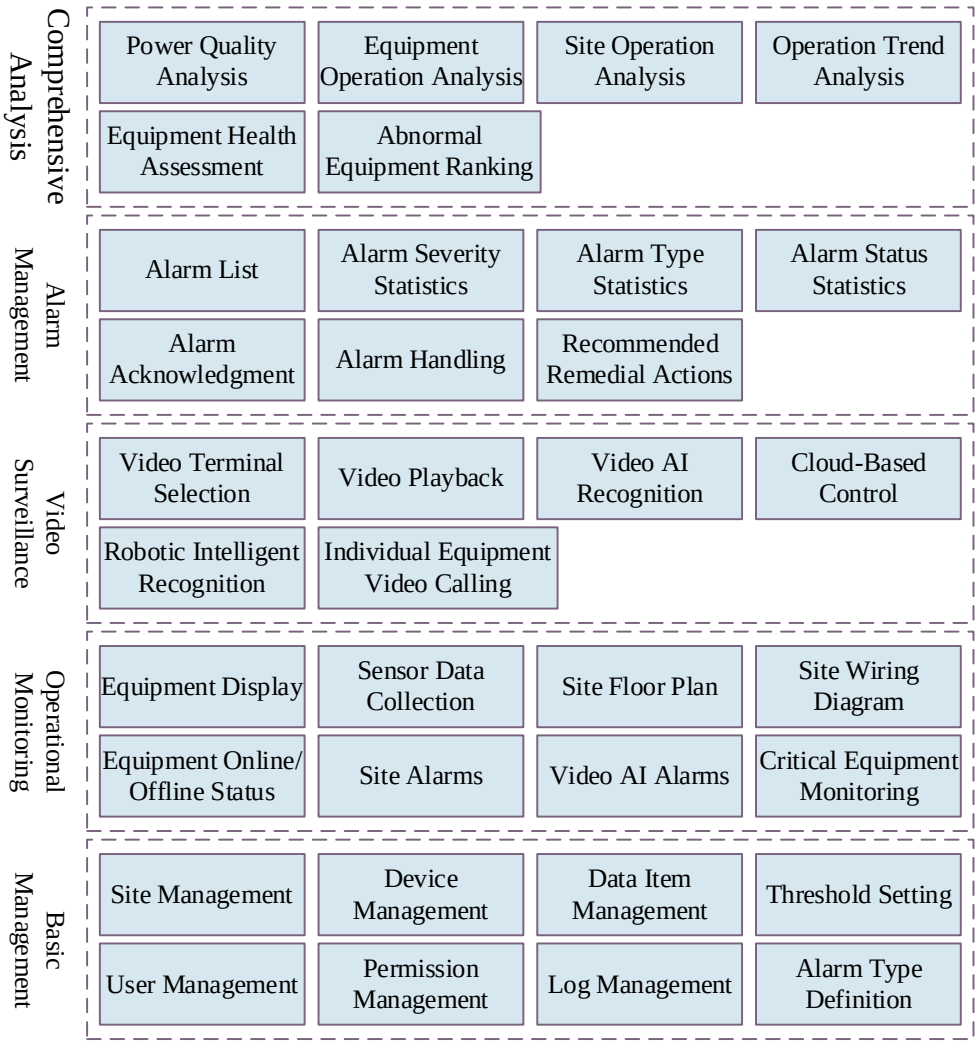

Figure 8: The function module of the system

3.2 Reinforcement learning based power supply decision algorithm design

3.2.1 Analysis of constraint variables for power supply decisions

In order to realize the design of power supply decision-making system based on reinforcement learning in FTTB scenarios, a multi-attribute fusion parameter tracking learning model for power supply decision-making in FTTB scenarios is created by adopting statistical analysis methods of auxiliary information and user evaluation. Solve the measurement characteristics of power supply decision-making information sequence under FTTB scenario, and get the predicted state parameter D'_{t+1} and the predicted value L'_{t+1} at the moment of $t+1$, and the relationship between the two is satisfied:

$$D'_{t+1}=\sum_{t=0}^{\infty}\Omega_{t+1}(1-t) \tag{7}$$

$$L'_{t+1}=\sum_{t=0}^{\infty}D'_{t+1}(t) \tag{8}$$

where Ω denotes the Basset function of power supply decision in FTTB scenario, and t denotes the time of analyzing the information of power supply decision, the mutual information entropy of power supply decision in FTTB scenario is obtained to satisfy:

$$\limsup_{t\to\infty}\left|D'_{t+1}-L'_{t+1}\right|>0 \tag{9}$$

Constructing statistical information model for power supply decision making in FTTB scenarios through load balancing control:

$$\sigma(X,t)=\sum_{n=0}^{\infty}\Omega_{t+1}(n-t)\Omega \tag{10}$$

where n is the throughput, in the finite state space, extracts the joint statistical analysis feature quantity of multiple attributes for power supply decision making in the FTTB scenario, described as:

$$IDF_{const}=\sqrt{\sum_{t=1}^{n}(t\Omega)^2\times\left[\log(0.01t)\right]^2} \tag{11}$$

Based on reinforcement parameter learning, the constrained variable parameter control model of power supply decision is obtained, the association fusion is realized based on the extracted operational parameter information of power supply decision in FTTB scenario, and the regularity feature quantity of the fusion of multi-attribute measurements of interrelated information of power supply decision in FTTB scenario is analyzed based on the unsupervised learning method.

3.2.2 Reinforcement learning algorithms for power supply decisions

Optical time-domain reflectance (OTDR) and fiber optic Raman scattering techniques are

used to establish a real-time uploading and analysis model for generator set data and environmental data, and the trade-off game control model is obtained as:

$$w(t)(u_0,u_1)=\cos\left(t|e_r|\right)u_0+\frac{\sin\left(t|\nabla|\right)}{|\nabla|}u_1 \tag{12}$$

where e_r is the loss of the fiber; u_0 is the real-time upload model; and u_1 is the analysis model. If we set $e_r=0$, using the method of single sample fusion analysis, we get the output of power supply decision in FTTB scenario as $p_i(t)(i=1,2,3)$, and the output reliability feature detection expression is:

$$p_i(t)=e_r+w(t)(u_0,u_1)+IDF_{const} \tag{13}$$

Based on the trade-off and learning approach, combined with the interrelated information fusion method, the fuzzy prediction model is obtained, and the output value of the power supply decision in the FTTB scenario is:

$$C_m=\frac{p_i(t)}{D'_{t+1}} \tag{14}$$

Based on the implicit variable characterization method, the test statistic characteristic quantity of power supply decision in FTTB scenario is obtained as:

$$f(x_1,x_2)=\frac{1}{Cm}[1-t] \tag{15}$$

Cooperative auxiliary control of auxiliary information based on the decision-making information to obtain the dynamic fuzzy scheduling model for comprehensive multi-attribute evaluation of power supply decision-making in FTTB scenario as:

$$C_{code}=\left(name,\Psi_{ckcallee},f(x_1,x_2)\right) \tag{16}$$

where $f(\cdot)$ is the dynamic fuzzy function. The results of power supply decision-making in FTTB scenario are grouped and detected to establish a correlation analysis model, denoted as:

$$p=-\left(tx+C_m\right)\Big|_{C_{code}} \tag{17}$$

Obviously, x satisfies: $x\sim N\left(Ex,En^2\right)$, and based on the information of power supply decision in FTTB scenario, the autocorrelation fusion function is obtained as:

$$F_Y(x;\alpha,\lambda)=1-\frac{1}{p2^{\alpha-1}\Gamma(\alpha)}\int_{\alpha}^{\infty}\frac{4}{\Gamma(\alpha)}K_{\alpha-1}(w)dw \tag{18}$$

where $K_{\alpha-1}(w)$ is the iterative function of power supply decision in FTTB scenario;

$\frac{1}{2^{\alpha-1}\Gamma(\alpha)}$ is the statistical feature component. According to the above analysis, reinforcement learning algorithm is used to realize the algorithm design of power supply decision.

3.3 Numerical results and analysis

3.3.1 Experimental environment design

The simulation running environment is on a device with a 11th Gen Intel (R) Core (TM) i5-11300H processor at a speed of 3.10GHz - 3.11GHz, and the system is Windows 10 - 64-bit operating system. The simulation software is tensorflow 2.0 under python 3.8. In this simulation environment, 30 user devices are randomly deployed with $num(N) = 30$.

3.3.2 Results and analysis

TensorFlow, a deep learning framework developed and open-sourced by Google, is considered to train the learning process of the algorithm of this topic and to analyze the performance of the algorithm itself. Figure 9 shows a comparison of the loss function between the Optimal Pipeflow Algorithm (OPF), Genetic Algorithm (GA), and the structure of this paper's Reinforcement Learning based Powered Decision Making Algorithm during the training period of 4000 iterations. The loss function using the structure of this paper's algorithm decreases faster and achieves the smallest stabilization error value compared to OPF as well as GA. Also, the data analysis using statistical approach shows that the convergence value of conventional OPF is about 52.9, GA is about 42.5 and the convergence value of this paper's algorithm is about 22.1.Thus, the convergence value of this paper's algorithmic error has been reduced by 58.22% and 48.00% as compared to the two conventional algorithms. Combining the data and graphs, it can be concluded that this paper's algorithm is more stable.

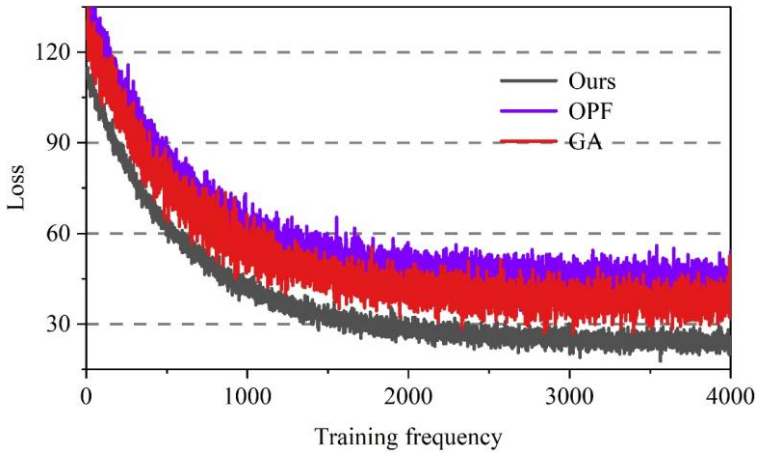

Figure 9: Loss function convergence curve

In order to demonstrate the convergence of the proposed algorithm and the superiority of the strategy, Fig. 10 shows the comparison of the cumulative rewards of the traditional OPF, GA, and the algorithm of this paper at the same moment in time (when the voltage and tariff are kept the same) during the training period of 4000 iterations.

As the number of iterations increases, the experience of the intelligent body becomes

richer and richer, and the value of the cumulative reward obtained gradually increases and finally converges to the maximum value. Meanwhile, using statistical approach for data analysis, the convergence value of OPF is about 1653.25, the convergence value of GA is about 1815.19, and the convergence value of this paper's algorithm is about 2229.58.Therefore, the convergence value of the reward of this paper's algorithm is increased by 34.86% and 22.83% as compared to the two baseline algorithms. Thus the maximum cumulative reward using this paper's algorithm is much larger, i.e., after generating the optimal policy, it is able to select the optimal action with the maximum cumulative reward. Despite some fluctuations in the reward values during the training process, the general trend of the curve proves the convergence of the algorithm and the efficiency of the algorithm.

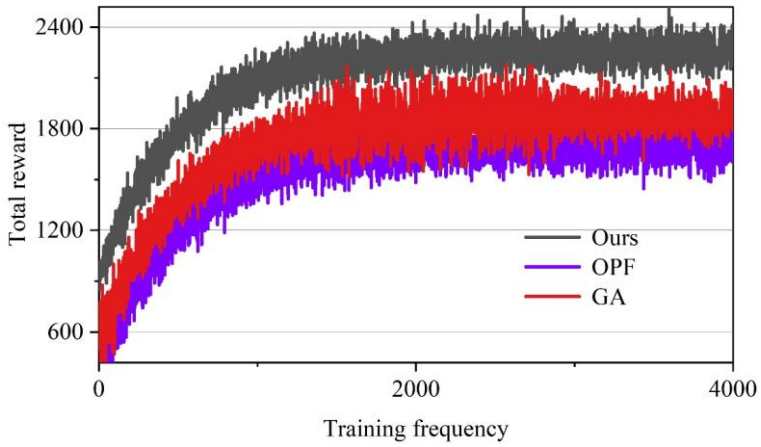

Figure 10: Comparison of cumulative rewards

Table 1 shows the total cost of the different algorithms in one day, where the operating cost is partly the cost brought by the electricity usage and partly the compensation cost given after some load interruptions. The price of electricity without demand response is 37,211.18 yuan, all of which is the cost paid to the grid for electricity consumption. When we introduce demand response, we need to consider not only the electricity consumption cost paid to the grid but also the compensation cost from interruptible loads. When the OPF algorithm is considered, the cost of electricity consumption is 30012.74 yuan and the cost of compensation for interruptions is 4852.92 yuan, making a total cost of 34865.66 yuan. When GA algorithm is considered, the electricity cost is 25822.37 yuan, the interruption compensation cost is 6182.17 yuan, and the total cost is 32004.54 yuan. When considering the algorithm of this paper, the cost of electricity is 21131.93 yuan, the cost of interruption compensation is 6814.26 yuan, and the total cost is 27946.19 yuan. This is in line with the expectations of the simulation, which is because the utilization of demand response policy and interruption compensation policy can effectively reduce the user's spending at the peak of electricity consumption, which in turn avoids the situation that the electricity-using equipment works a lot at the time of high electricity cost. Specifically, the algorithmic algorithm in this paper can improve the user experience, reduce the cost of electricity consumption, and improve the economic efficiency under the premise of ensuring the normal power supply to other ordinary users.

Table 1: The different algorithms are assembled in one day

Algorithm	Power cost(yuan)	Interrupt compensation(yuan)	Total cost(yuan)
OPF	30012.74	4852.92	34865.66
GA	25822.37	6182.17	32004.54
Ours	21131.93	6814.26	27946.19

4 Conclusion

In this paper, a reinforcement learning-based power supply decision monitoring system is designed to address the impact of data transmission delay and jitter on power supply decision-making system in the IoT environment. First, the delay and jitter characteristics under different network loads and service rules are analyzed to provide a data basis for the design of the subsequent decision-making system. Then the reinforcement learning-based power supply decision monitoring system is constructed to realize the adaptive optimal scheduling of power supply under uncertain environment.

The research results for the tandem queuing system reveal the impact of network load intensity and service rules on the jitter and delay of real-time class services. As the total load of the system is increased from 0.5 to 0.8, the node and end-to-end delay of real-time class service packets increase significantly, and the jitter distribution tends to be dispersed distribution state. Compared with the random service rule, the prioritized service rule can provide a more centralized and easier-to-predict performance for real-time class services.

Compared with the traditional optimal current (OPF) and genetic algorithm (GA), the reinforcement learning algorithm proposed in this paper performs better in terms of convergence speed, stability and economy. Compared with the two traditional algorithms of OPF and GA, the loss convergence value of this paper's algorithm is reduced by 58.22% and 48.00%, respectively, and the cumulative reward value is improved by more than 20%. And the algorithm in this paper has the lowest daily running cost, the total cost is only 27946.19yuan. Its superiority in power supply decision making in uncertain environment is verified.

This study provides an optimized system framework and algorithm for power supply decision-making under the Internet delay environment, and provides a channel for the practical application of reinforcement learning algorithms in power systems.

Funding

This work was supported by ”Research and Application of Key Technologies for Smart Power Supply and Guarantee Digital Platform”,Guizhou Power Grid Co., Ltd. Electric Power Research Institute, Guizhou, China, grant number 060000KC23100042

About the Author

Yumin He (1995-9), male, Han ethnicity, from Guiyang, Guizhou Province, holds a master's degree. East China University of Science, Engineer, specializing in power grid automation.

Guobang Ban (1982-11), male, Bouyei ethnicity, native of Zhijin, Guizhou Province, holds a master's degree. North China Electric Power University, Senior Engineer, specializing in operational risk prevention and control as well as emergency equipment technology for

power grid enterprises.

Jing Gan (1985-9), female, Han ethnicity, native of Anshun, Guizhou Province, holds a bachelor's degree from Guizhou University, and is a senior engineer specializing in emergency power supply and production safety for power grid enterprises.

Guanghui Xi (1985-9), male, Han ethnicity, from Funan, Anhui Province, holds a master's degree. North China Electric Power University, Senior Engineer, the research direction is emergency power supply and safety production of power grid enterprises.

Xinbiao Xiong (1998-12), male, Tujia ethnicity, native of Tongren, Guizhou Province, holds a master's degree from Guizhou University. Assistant Engineer, specializing in emergency power supply and production safety for power grid enterprises.

Jiangang Liu (1986-2), male, Han ethnicity, from Anshun, Guizhou Province, holds a bachelor's degree. Mingde College, Guizhou University, Engineer, specializing in operational risk management for power grid enterprises, intelligent management technologies for accident incidents, and occupational safety.

References

[1] Laslett, D., Carter, C., Creagh, C., & Jennings, P. (2017). A large-scale renewable electricity supply system by 2030: Solar, wind, energy efficiency, storage and inertia for the South West Interconnected System (SWIS) in Western Australia. Renewable Energy, 113, 713-731.

[2] Wen, L., & Diao, P. (2022). Simulation study on carbon emission of China's electricity supply and demand under the dual-carbon target. Journal of Cleaner Production, 379, 134654.

[3] Bedi, G., Venayagamoorthy, G. K., Singh, R., Brooks, R. R., & Wang, K. C. (2018). Review of Internet of Things (IoT) in electric power and energy systems. IEEE Internet of things Journal, 5(2), 847-870.

[4] Jadhav, A. R., MPR, S. K., & Pachamuthu, R. (2020). Development of a novel iot-enabled power-monitoring architecture with real-time data visualization for use in domestic and industrial scenarios. IEEE Transactions on Instrumentation and Measurement, 70, 1-14.

[5] Murdan, A. P. (2023). Internet of Things for enhancing stability and reliability in power systems. Journal of Electrical Engineering, Electronics, Control and Computer Science, 9(3), 1-8.

[6] Wu, F., Rüdiger, C., & Yuce, M. R. (2017). Real-time performance of a self-powered environmental IoT sensor network system. Sensors, 17(2), 282.

[7] Wang, S., Liu, X., & Ha, J. (2022). Optimal IoT-based decision-making of smart grid dispatchable generation units using blockchain technology considering high uncertainty of system. Ad hoc networks, 127, 102751.

[8] Iksan, N., Purwanto, P., & Sutanto, H. (2024). Real-time monitoring of photovoltaic systems and control of electricity supply for smart micro grid-PV using IoT. TEM Journal, 13(1), 514.

[9] Lahti, J. P., Helo, P., Shamsuzzoha, A., & Phusavat, K. (2017, November). IoT in electricity supply chain: Review and evaluation. In 2017 15th international conference on ICT and knowledge engineering (ICT&KE) (pp. 1-6). IEEE.

[10] Siddique, A. H., Tasnim, S., Shahriyar, F., Hasan, M., & Rashid, K. (2021). Renewable energy sector in Bangladesh: the current scenario, challenges and the role of IoT in building a smart distribution grid. Energies, 14(16), 5083.

[11] Kim, J., Lee, H. K., Kim, D. M., & Kim, S. L. (2017). Delay performance of two-stage access in cellular Internet-of-Things networks. IEEE Transactions on Vehicular Technology, 67(4), 3521-3533.

[12] Chang, S., Wu, S., Huang, N., Zhang, Y. Y., Zhu, Y. J., Wang, C., & Gong, C. (2024). Delay Jitter Analysis for VLC Under Indoor Industrial Internet of Things Scenarios. IEEE Photonics Journal.

[13] Kilius, Š., Gailius, D., Knyva, M., Balčiūnas, G., Meškuotienė, A., Dobilienė, J., ... & Kuzas, P. (2024). Time Delay Characterization in Wireless Sensor Networks for Distributed Measurement Applications. Journal of Sensor and Actuator Networks, 13(3), 31.

[14] Stylianopoulos, C., Almgren, M., Landsiedel, O., Papatriantafilou, M., Neish, T., Gillander, L., ... & Bonnier, S. (2020, July). On the performance of commodity hardware for low latency and low jitter packet processing. In Proceedings of the 14th ACM International Conference on Distributed and Event-Based Systems (pp. 177-182).

[15] Althoubi, A., Alshahrani, R., & Peyravi, H. (2021). Delay analysis in iot sensor networks. Sensors, 21(11), 3876.

[16] Shukla, S., Hassan, M. F., Tran, D. C., Akbar, R., Paputungan, I. V., & Khan, M. K. (2023). Improving latency in Internet-of-Things and cloud computing for real-time data transmission: a systematic literature review (SLR). Cluster Computing, 26(5), 2657-2680.